Biol Cybern (2009) 101:71–80
DOI 10.1007/s00422-009-0318-5

ORIGINAL PAPER

Biological Cybernetics

Short-window spectral analysis using AMVAR and multitaper methods: a comparison

Hariharan Nalatore · Govindan Rangarajan

Received: 6 October 2008 / Accepted: 6 May 2009 / Published online: 27 May 2009
© Springer-Verlag 2009

Abstract We compare two popular methods for estimating the power spectrum from short data windows, namely the adaptive multivariate autoregressive (AMVAR) method and the multitaper method. By analyzing a simulated signal (embedded in a background Ornstein–Uhlenbeck noise process) we demonstrate that the AMVAR method performs better at detecting short bursts of oscillations compared to the multitaper method. However, both methods are immune to jitter in the temporal location of the signal. We also show that coherence can still be detected in noisy bivariate time series data by the AMVAR method even if the individual power spectra fail to show any peaks. Finally, using data from two monkeys performing a visuomotor pattern discrimination task, we demonstrate that the AMVAR method is better able to determine the termination of the beta oscillations when compared to the multitaper method.

Keywords Spectral analysis · AMVAR method · Multitaper method

1 Introduction

The power spectrum of most signals encountered in practice change with time as the signals are typically non-stationary. These signals include neurobiological signals, speech signals, etc. Since the nature of the signal changes rapidly even over time intervals of the order of one second, one must examine them using short time windows of 50–100 ms duration or even shorter. The theoretical basis for dividing the signal into short time windows lies in treating the time series within such short windows as being generated by an approximately stationary stochastic process. In other words, the full time series is viewed as being generated by a non-stationary stochastic process with locally stationary segments.

For the 200 Hz sampling frequency used in our study, a duration of 50–100 ms corresponds to a data string of only 11–21 points. The conventional non-parametric approach to spectral analysis, based on the discrete Fourier transform, is not effective for such short data lengths. Even with the help of advanced windowing techniques, older non-parametric methods produce highly biased spectral estimates for these short data lengths (Granger and Hughes 1968; Jenkins and Watts 1968; Percival and Walden 1993; Muthuswamy and Thakor 1998). In this paper, we compare the performance of two recent methods when analyzing such short data lengths: The parametric adaptive multivariate autoregressive (AMVAR) method and the non-parametric multitaper method. Earlier papers (Spyers-Ashby et al. 1998; Muthuswamy and Thakor 1998) have shown that the AMVAR method is superior to the conventional FFT methods. Similarly, the multitaper method has been shown to be better than conventional non-parametric methods (Mitra and Pesaran 1999; Walden 2000).

In Sect. 2, we briefly describe the AMVAR and multitaper methods. In Sect. 3, we describe our numerical model of signal plus noise. In Sect. 4, using the above model we compare the performance of the AMVAR and multitaper methods for short data lengths. In Sect. 5, we analyze LFP data recorded from the somatosensory area of two monkeys (LU and GE). We again compare the performance of AMVAR and

H. Nalatore
Applied Research International, B1-Haus Khas, New Delhi, India
e-mail: hariharan.nalatore@gmail.com

G. Rangarajan (✉)
Department of Mathematics, Centre for Neuroscience,
Indian Institute of Science, Bangalore, India
e-mail: rangaraj@math.iisc.ernet.in

multitaper methods in determining the termination of bursts of oscillations. Our conclusions are given in Sect. 6.

2 Theoretical considerations

Consider a neurobiological signal recorded using p channels. We model this using a p-dimensional zero mean stationary stochastic process X:

$$\mathbf{X}(t) = [X(1,t), X(2,t), \ldots, X(p,t)]^{\mathrm{T}}, \tag{1}$$

where T denotes the matrix transposition.

First, we define the elements of the spectral matrix $\mathbf{S}$ for this process as (Jenkins and Watts 1968)

$$S_{lm}(f) = \sum_{\tau} C_{lm}(\tau) \mathrm{e}^{(-i2\pi f\tau)}, \quad 1 \le l, m \le p, \tag{2}$$

where $C_{lm}(\tau)$ denotes the cross-covariance function between channels l and m at lag τ:

$$C_{lm}(\tau) = \mathrm{E}\{X^*(l,t)X(m,t+\tau)\}.$$

Here E{} denotes the expectation and $f \in [0, f_N]$, where f_N is the Nyquist frequency. The asterisk denotes the Hermitean conjugation. When $l = m$, $S_{ll}(f)$ gives the autospectrum of the lth channel. For $l \neq m$, one gets the cross-spectrum between channels l and m.

The (ordinary) coherence (also called "squared coherency") between a pair of channels l and m is defined by (Jenkins and Watts 1968)

$$\mathrm{Coh}_{lm}(f) = \frac{|S_{lm}(f)|^2}{S_{ll}(f)S_{mm}(f)} \tag{3}$$

provided $S_{ll}(f) \neq 0$ and $S_{mm}(f) \neq 0$. It is a measure of interdependence between channel l and channel m at frequency f. Its value ranges from 0 to 1. If $\mathrm{Coh}_{lm}(f)$ is close to 1, then there is a maximum interdependence between channel l and channel m; if $\mathrm{Coh}_{lm}(f)$ is close to 0, it indicates no interdependence.

2.1 AMVAR method

Here, we briefly recollect the AMVAR method introduced in Ding et al. (2000) for estimating spectral quantities.

AMVAR modeling can be used as a parametric spectral analysis technique. Here multivariate autoregressive (MVAR) time series models are adaptively extracted from the data which becomes the basis for deriving spectral quantities. First, we choose a sliding window of suitable length. The stochastic process $\mathbf{X}(t)$ (cf. Eq. 1) is modeled as a MVAR process of order M:

$$\sum_{k=0}^{M} \mathbf{A}_k \mathbf{X}(t-k) = \mathbf{Z}(t). \tag{4}$$

Here $\mathbf{Z}(t)$ is a zero mean uncorrelated $p \times 1$ noise vector with a $p \times p$ covariance matrix Σ and $\mathbf{A}_k$ are $p \times p$ coefficient matrices that are obtained by solving the multivariate Yule–Walker equations using the Levinson, Wiggins and Robbinson (LWR) algorithm (Morf et al. 1978). We define A_0 to be the identity matrix.

The model order M is determined by minimizing the Akaike Information Criterion (AIC) (Marple 1987) given by

$$\mathrm{AIC}(M) = 2\log[\det(\Sigma)] + \frac{2p^2M}{N_{\mathrm{total}}}, \tag{5}$$

where N_{total} is the total number of data points from all trials. The data from several trials are considered as the realizations of the same underlying stationary stochastic process and are combined to produce the estimation of the model coefficients. The term adaptive refers to the fact that the above procedure is repeated for each analysis window along the time course of the data.

Once the model coefficients $\mathbf{A}_k$ and Σ are estimated, the spectral matrix is estimated as (cf. Eq. 2)

$$\hat{\mathbf{S}}(f) = \mathbf{H}(f)\hat{\Sigma}\mathbf{H}^*(f), \tag{6}$$

where

$$\mathbf{H}(f) = \frac{1}{\left(\sum_{j=0}^{M} \hat{\mathbf{A}}_j \mathrm{e}^{-2\pi ijf}\right)}$$

is the transfer function of the system and $\hat{\mathbf{A}}$, $\hat{\Sigma}$ denote the estimated quantities.

2.2 Multitaper method

The multitaper method for estimating the power spectrum was proposed by Thomson (1982) and is known to have several advantages over other non-parametric spectral methods (Percival and Walden 1993; Mitra and Pesaran 1999; Percival and Walden 2000; Walden 2000). A brief description of this method follows. Consider a stationary process $\mathbf{X}(t)$. Let the sampling interval between observations be Δt, so that the Nyquist frequency is $f_N = 1/(2\Delta t)$. The multitaper spectral estimator (Thomson 1982) utilizes several different data tapers which are orthogonal to each other. The multitaper cross-spectral estimator between channel l and m is the average of K direct cross-spectral estimators between the same pair of channels (l and m) and hence takes the form

$$\hat{S}^{lm}(f) = \frac{1}{K}\sum_{k=0}^{K-1} \hat{S}_k^{lm}(f). \tag{7}$$

Here, $\hat{S}_k^{lm}(f)$ is the kth direct cross spectral estimator between channel l and m and is given by

$$\hat{S}_k^{lm}(f) = \frac{1}{N\Delta t}[J_k^l(f)]^*[J_k^m(f)],$$

where

$$J_k^l(f) = \sum_{t=1}^{N} h_{t,k} X(l,t) \mathrm{e}^{-i2\pi f t \Delta t}.$$

Here, $k = 0, 1, 2, 3, \ldots, K$. The sequence $\{h_{t,k}\}$ is the data taper for the kth direct cross-spectral estimator $\hat{S}_k^{lm}(f)$ and is chosen as follows.

We choose a set of K orthogonal data tapers such that each one provides good protection against leakage. These are given by the discrete prolate spheroidal sequences (dpss) (Slepian and Pollak 1961) with parameter W and orders $k = 0$ to $K-1$. The maximum order K is chosen to be less than the Shannon number $2NW\Delta t$. The quantity $2W$ defines the resolution bandwidth for the concentration problem (Percival and Walden 1993) and $W \in (0, f_N)$. When $l = m$ in Eq. (7), we get the multitaper estimator for the auto-spectrum of the lth channel.

In conventional non-parametric spectral analysis techniques, to reduce variance, we break up the data into overlapping segments (as in Welch's overlapped segment method), estimate the cross-spectrum or power spectrum for each segment and then average over the segments. Such methods have severe bias problems for short data. In the multitaper method, for reducing variance we average over different tapers using the full data. Since the data length is not shortened, bias is smaller.

The following is the general approach we follow to perform spectral analysis of non-stationary signals:

1. Cover the time series data using highly overlapped time windows each of which is short enough that the process in each window can be treated as locally stationary.
2. In the AMVAR method, for each time window, derive a linear stochastic MVAR model of the process by fitting the data from an ensemble of trials. Derive the power and coherence from the model parameters. By adaptively fitting models over successive windows, obtain the temporal evolution of these spectral quantities.
3. In the multitaper method, for each time window, derive the power and coherence using multitaper spectral estimators from an ensemble of trials. The evaluation of these spectral quantities over successive windows as the analysis window slides along the time axis gives their temporal evolution.

3 Numerical experiments

We first compare the two methods using numerical experiments. The time series to be analyzed is generated as follows. The signal part is obtained using a coupled neuron model. The background noise is modeled using an Ornstein–Uhlenbeck (OU) process. The final time series data is obtained by superimposing a short segment of the signal over the background noise.

3.1 Generation of the signal

Our simulation model comprises two coupled cortical columns where each column is made up of an excitatory and an inhibitory neuronal population (Kaminski et al. 2001). The equations governing the dynamics of the two columns are given by

$$\ddot{x_i} + (a+b)\dot{x_i} + abx_i = -k_{ei} Q(y_i(t), Q_{m0}) + k_{ij} Q(x_j(t), Q_{m0}) + \xi_{x_i}(t), \quad (8)$$

$$\ddot{y_i} + (a+b)\dot{y_i} + aby_i = k_{ie} Q(x_i(t), Q_{m0}) + \xi_{y_i}(t), \quad (9)$$

where $i \neq j = 1, 2$. Here x and y represent local field potentials (LFP) of the excitatory and inhibitory populations, respectively, $k_{ie} > 0$ gives the coupling gain from the excitatory (x) to the inhibitory (y) population, and $k_{ei} > 0$ is the strength of the reciprocal coupling. The neuronal populations are coupled through a sigmoidal function $Q(x, Q_{m0})$ which represents the pulse densities converted from x with Q_{m0} a modulatory parameter. The function $Q(x, Q_{m0})$ is defined by,

$$Q(x, Q_{m0}) = \begin{cases} Q_{m0}[1 - \mathrm{e}^{-(\mathrm{e}^x - 1)/Q_{m0}}], & \text{if } x > -u_0, \\ -1, & \text{if } x \leq -u_0, \end{cases}$$

where $u_0 = -\ln[1 + \ln(1 + \frac{1}{Q_{m0}})]$. The coupling strength k_{np} is the gain from the excitatory population of column p to the excitatory population of column n, with $k_{np} = 0$ for $n = p$. The terms $\xi(t)$ represent independent Gaussian white noise inputs given to each neuronal population. These vary from trial to trial.

The above system of equations was integrated to get $x_1(t)$ for $t \in [0s, 1s]$. The initial conditions for x and y are kept fixed across trials. The integration step size was 5 μs and the whole data was down sampled to 200 Hz. All simulations were implemented using Matlab. The parameter values used were: $a = 0.22$/ms, $b = 0.36$/ms, $k_{ie} = 0.1, k_{ei} = 0.4, k_{12} = 0, k_{21} = 0.1$ and $Q_{m0} = 5$. The variance for the Gaussian white noise was chosen as 0.01. Three hundred realizations of the signal $x_1(t)$ were generated. This signal is a stationary signal and for the above set of parameters it has a peak around 41 Hz in the power spectrum.

3.2 Generation of OU noise

An OU process is generated by

$$\dot{x}(t) = -\lambda x(t) + \xi(t), \quad (10)$$

where λ is a parameter independent of time t and the driving function $\xi(t)$ is a Gaussian white noise with mean zero and

variance σ^2. The quantity $\tau = 1/\lambda$ is called the relaxation time of the process. This is a continuous, stationary Markov process. We use this process as a model for background noise.

The above equation can be integrated using an exact update formula (see Gillespie 1996) given by (for $m = 1, 2, \ldots$)

$$x_{m+1} = x_m e^{-\lambda s} + \left\{ \frac{\sigma^2}{2\lambda}[1 - e^{-2\lambda s}] \right\}^{1/2} N(0, 1), \qquad (11)$$

where $N(0, 1)$ is the sample value of the Gaussian random number generator with mean 0 and variance 1. This update formula is independent of the choice of the step size s used in the integration of Eq. (10). The theoretical one sided power spectrum of the OU process is given by (see Bartosch 2001)

$$S(f) = \frac{2\sigma^2}{\lambda^2 + (2\pi f)^2}.$$

Thus, the power spectrum of an OU process decreases monotonically from its maximum value at $f = 0$. Therefore, it contains stronger contributions from lower frequencies than from higher frequencies. Hence, an OU process is also referred to as Gaussian red noise.

We generated 300 realizations of the OU noise. For each realization, the integration step size was 0.1 ms and the data was down sampled to 200 Hz. The parameters used were $\lambda = 0.1$, $\sigma = 1.4$ and 3. The lower (higher) values of σ were used to generate a time series with higher (lower) signal-to-noise ratios.

3.3 Signal embedded in noise

The time series to be analyzed was generated as follows. We start with a realization of the original signal $x_1(t)$. We randomly cut a portion of this signal with a window length of L_w (e.g. $L_w = 150$ ms). This chopped signal is weighted using a sine window function and is then embedded in a realization $z(t)$ of OU noise (1 s long) at the center (500 ms along time axis). Mathematically, this can be expressed as (for $k = 1, 2, \ldots, 201$):

$$f(t_k) = z(t_k) + w(t_k)x_1(t_k), \quad \text{if } k = 101, \ldots 101 + m_w;$$
$$= z(t_k), \quad \text{otherwise},$$

where $t_k = (k - 1)s$, $s = 5$ ms, $m_w = [L_w/s]$, $w(t_k) = \sin(\pi(k - 101)/m_w)$. Here $[L_w/s]$ stands for the integer part of L_w/s. For obtaining 300 different realizations of the data, we randomly chopped different portions of the signal using the same window length L_w and embedded it in 300 different realizations of the OU noise as described above. Consequently, we get a collection of 300 realizations of the combined non-stationary time series. A typical plot of one realization of the combined process is shown in Fig. 1. The individual power spectra of the signal and noise separately

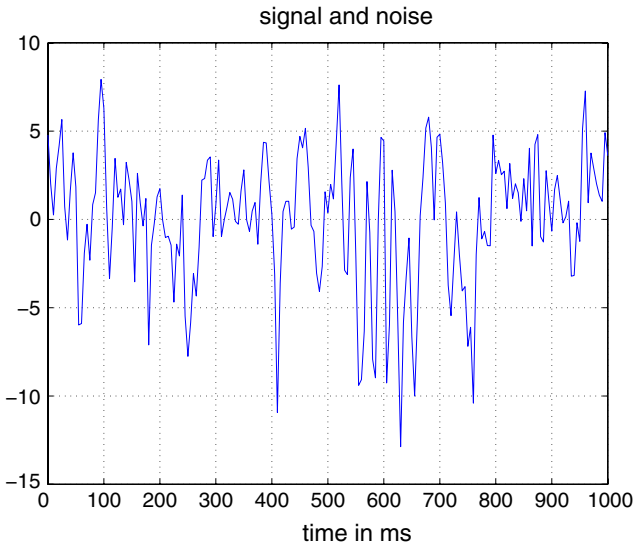

Fig. 1 A representative realization of the combined process (signal plus noise)

are shown in Fig. 2. The OU noise spectrum corresponds to that of an $1/f^2$ curve. The power spectrum corresponding to the pure signal shows a peak at 41 Hz as mentioned earlier.

The combined signal plus noise data was analyzed using the AMVAR and the multitaper methods. For the multitaper method, the standard routine included in Matlab was used. For the AMVAR method, an algorithm based on LWR method was used. Since the combined process is non-stationary, we chose an analysis window which slides over the time series data. The time series data within this analysis window was considered to be stationary. In each window, the data from all realizations was used to estimate the power spectrum by both methods. The length of the analysis window for each of the two methods was chosen so as to optimize performance, i.e. an appropriate combination of the two spectra given in Fig. 2 should be observed depending on the location of the window along the time axis.

4 Comparison of AMVAR and multitaper methods

4.1 Power spectrum analysis

The AMVAR analysis was performed using sliding windows of length 50 ms (11 time points), 100 ms (21 time points) and 150 ms (31 time points) and with a model order $M = 4$ in accordance with the Akaike Information Criterion (Eq. 5). The multitaper analysis was performed using the same sliding window lengths and with a time bandwidth product $NW\Delta t = 2$. This value of NW gives a better frequency resolution for the multitaper method. In both methods, the analysis

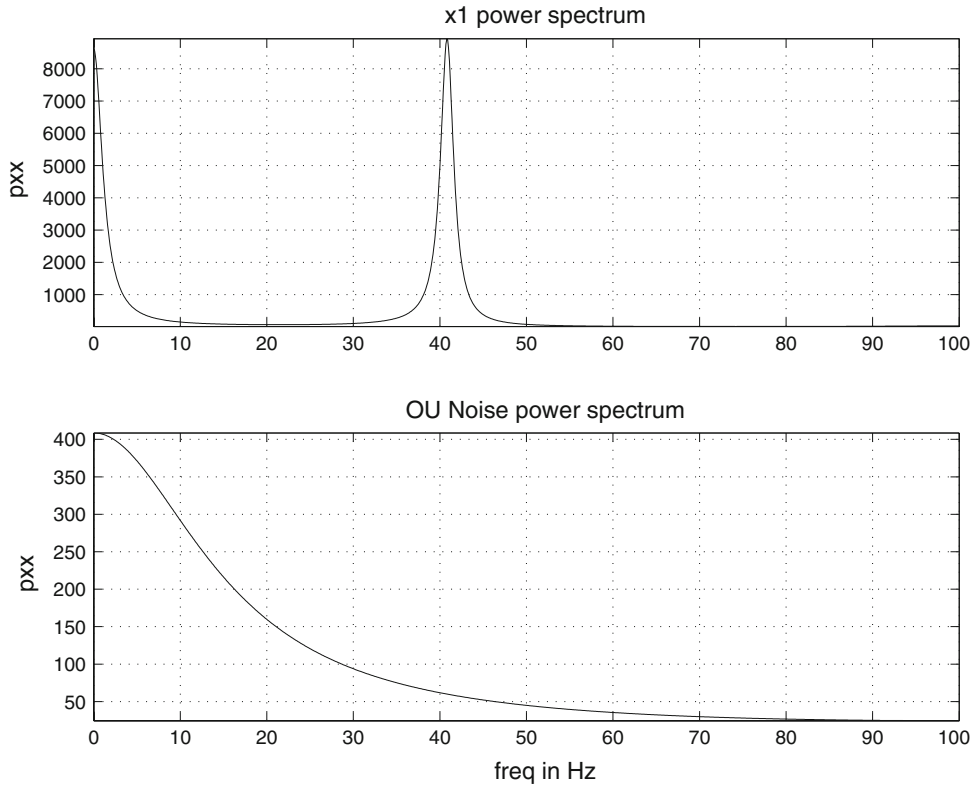

Fig. 2 The power spectra of the signal $x_1(t)$ and the OU noise process

window was moved from 400 to 725 ms along the time axis of the data.

For long signals (large L_w) embedded in noise, the qualitative features of the power spectra estimated using the AMVAR method remained the same irrespective of the sliding window length. For short signal lengths, 50 ms sliding window gave better results. On the other hand, multitaper method with 150 ms sliding window gave the best frequency resolution.

For a sufficiently long signal ($L_w = 150$ ms) embedded in OU noise, both AMVAR and multitaper methods were able to recover the signal as shown in Fig. 3. But the frequency resolution of AMVAR was better than that of the multitaper method. When L_w was decreased to 75 ms, both methods still detected the signal.

When L_w was reduced further to 50 ms, AMVAR (using a 50 ms analysis window) succeeded in detecting the signal satisfactorily while the multitaper method failed to capture the signal (see Fig. 4). When L_w was reduced further to 25 ms, AMVAR still detected the signal. However, the frequency resolution was poorer.

4.2 Jitter analysis

Here, we varied the time point where the signal is embedded in OU noise from trial to trial. In our study, a randomly selected signal of length $L_w = 100$ ms was embedded in OU noise using a small jitter. The jitter length was 30 ms in one case and 70 ms in the other. This signal plus noise time series was then analyzed using the AMVAR and the multitaper methods with a 150 ms sliding window. Both the methods were able to capture the signal in their power spectrum despite the introduction of jitter as shown in Fig. 5 (for jitter length of 70 ms). Of course, as L_w is decreased, the AMVAR method performed better compared to the multitaper method as seen in the previous section.

The reason for the success of the methods even when jitter is present is easily understood by considering the manner in which the power spectra are estimated by the two methods. In the AMVAR method, the reflection coefficients are first determined using the time series for each trial. These reflection coefficients are then averaged over all realizations and used to estimate the model coefficients. Likewise, in the multitaper method, the power spectrum was determined for each trial and only then averaged over all realizations. Since both the methods evaluate key quantities on a trial by trial basis before performing the ensemble average, introduction of jitter does not degrade their performance.

4.3 Coherence analysis

We now use the AMVAR and the multitaper methods to investigate a related issue. If there is strong coherencepres-

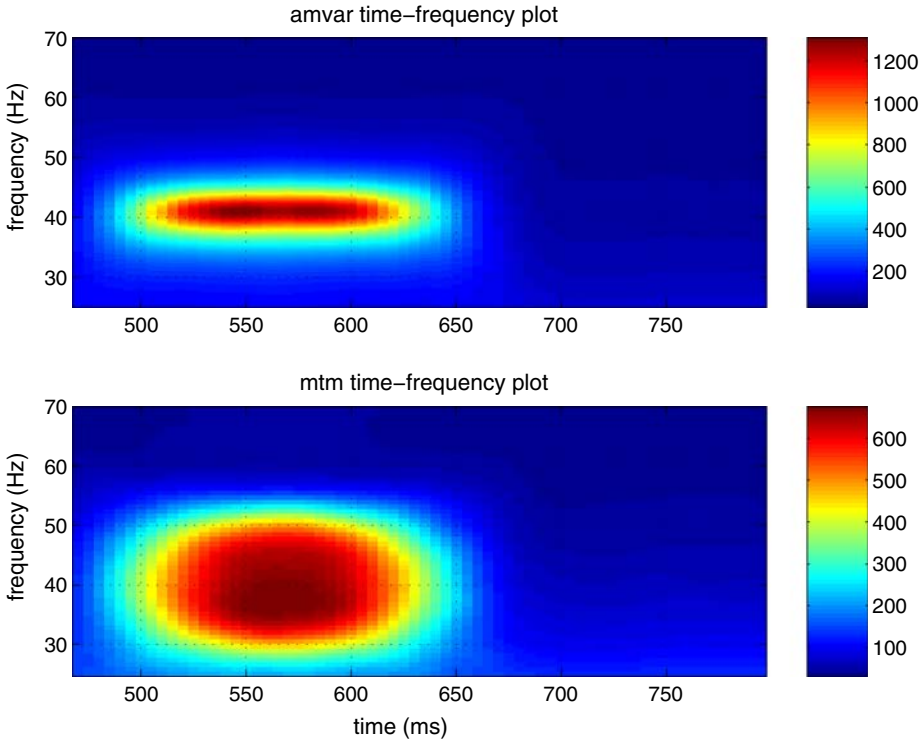

Fig. 3 The time–frequency plots of power spectra using AMVAR and multitaper methods with $L_w = 150\,\text{ms}$

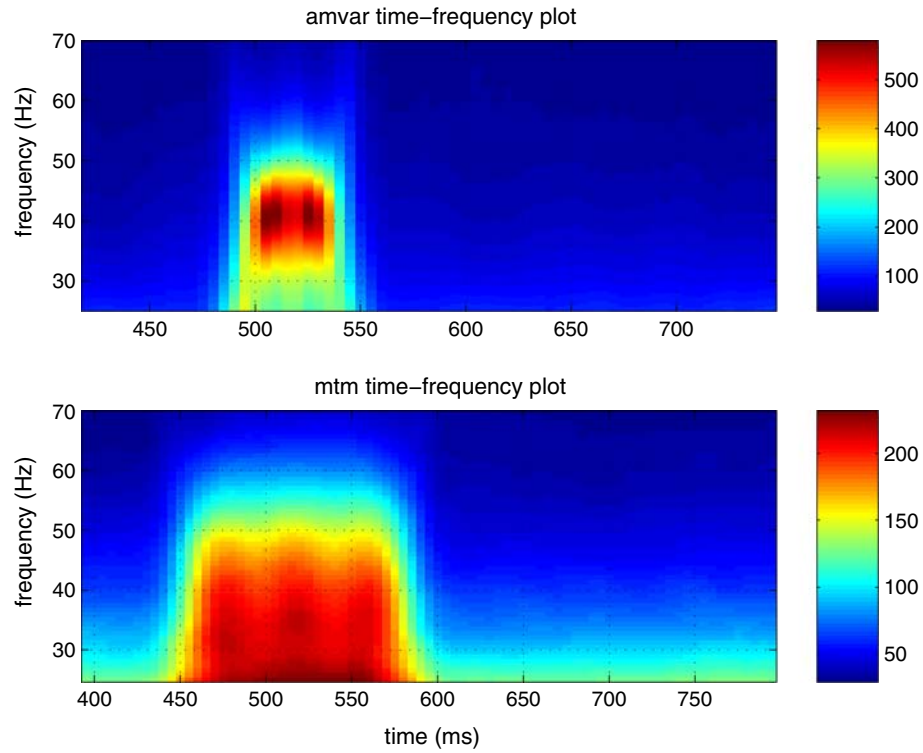

Fig. 4 The time–frequency plots of power spectra using AMVAR and multitaper methods with $L_w = 50\,\text{ms}$

ent between two noisy channels at a given frequency, is this coherence more easily detectable compared to peaks at this frequency in the individual power spectra?

To investigate this, 300 realizations of signal plus noise were taken from two different channels and coherence between them was computed. The noises present in the two channels were independent of each other. We used $L_w = 100\,\text{ms}$ and analyzed the data using AMVAR and multitaper method with a sliding window of length 50 and 150 ms, respectively.

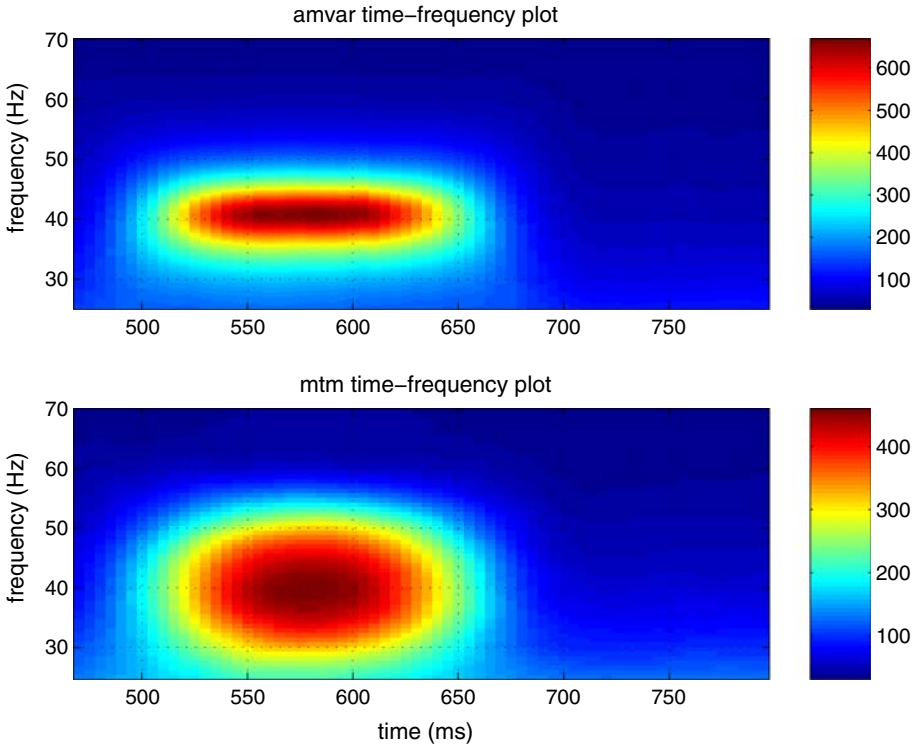

Fig. 5 The time–frequency plots of power spectra using AMVAR and multitaper methods with jitter length 70 ms and $L_w = 100$ ms

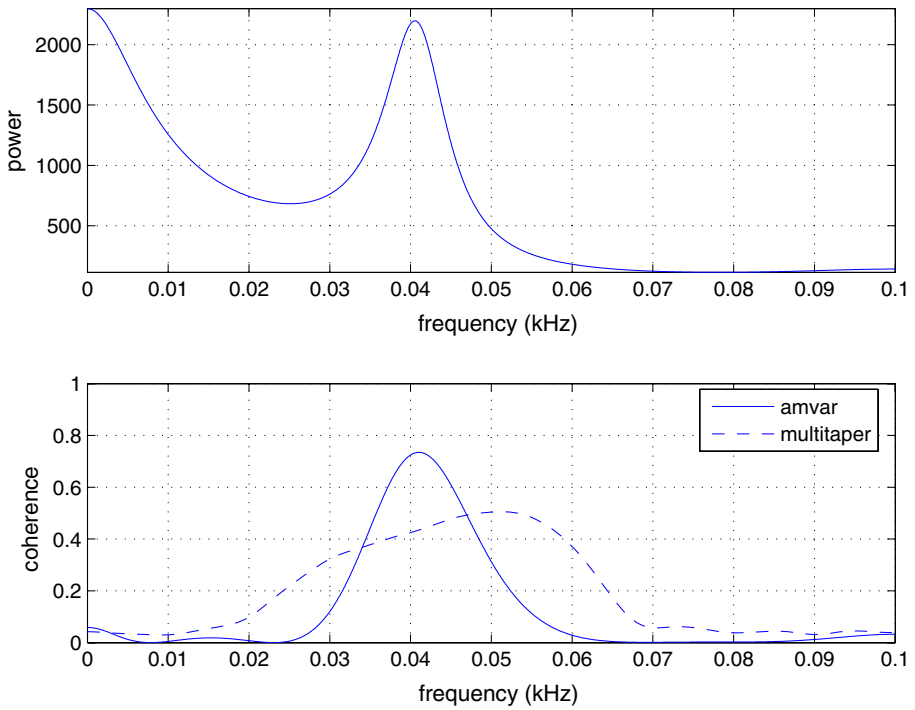

Fig. 6 The *top panel* gives the power spectrum for one of the two noisy channels with low background noise level ($\sigma = 3.0$). The *bottom panel* compares the coherence obtained for the same data using the AMVAR method (*solid line*) and the multitaper method (*dashed line*)

For a low value of the background OU noise ($\sigma = 3$), the power spectra of both channels show a peak at 41 Hz. The result for one channel is shown in Fig. 6. The coherence spectrum of these channels shows a nice peak at the same frequency when the AMVAR method is used while the multitaper method gives a much broader peak (Fig. 6). When the background noise level was increased ($\sigma = 5$) in both the channels, the power spectra barely show the peak at 41 Hz as seen from Fig. 7. The coherence spectrum obtained using the AMVAR method has a clear peak at 40.75 Hz. On the other hand, the multitaper method fails to capture this peak (Fig. 7). When the noise level was increased even further

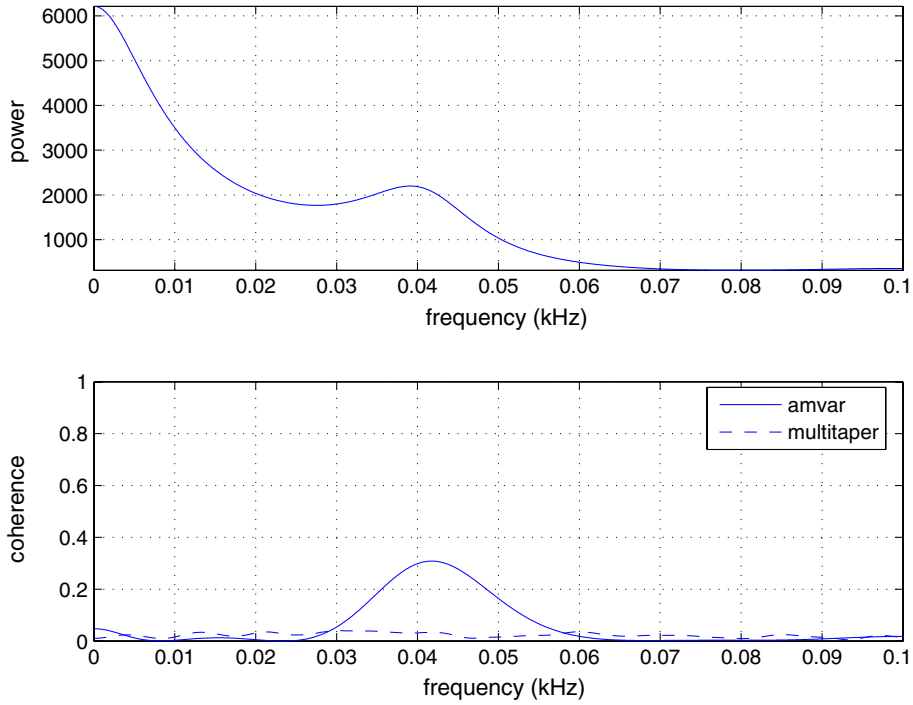

Fig. 7 The *top panel* gives the power spectrum for one of the two noisy channels with higher background noise level ($\sigma = 5.0$). The *bottom panel* compares the coherence obtained for the same data using the AMVAR method (*solid line*) and the multitaper method (*dashed line*)

($\sigma = 7.5$) the power spectrum does not show the signal while the coherence spectrum using AMVAR shows a peak at around 43 Hz.

4.4 Signal duration analysis

In this section, we estimate the duration of the embedded oscillatory signal. The analysis window was chosen to be 5 and 150 ms long for the AMVAR and it was moved along the time axis by one data point for the time series (signal plus noise). In multitaper method a 150 ms analysis window was used since shorter analysis windows failed to capture the signal.

The duration of the embedded signal is computed as follows. In both methods, as the analysis window slides, the power spectrum evolves with time as the window approaches and recedes from the embedded signal. As the window approaches the signal, the time (t_i) corresponding to the leading edge of that analysis window in which the peak in the power spectrum first shows up is noted. Since at least one cycle of the signal needs to be present in the analysis window in order to detect the peak, we correct t_i by subtracting from it the time period of the signal (25 ms). When the window recedes from the signal, the time (t_f) corresponding to the trailing edge of that analysis window in which the peak in the power spectrum first disappears is noted. By the same argument as above, we correct t_f by adding one time period of the signal. The difference between these corrected times gives the duration of signal.

Table 1 Duration of signal as estimated by AMVAR and multitaper methods

Actual duration (ms)	Duration by AMVAR method (ms)	Duration by multitaper method (ms)
150	130	80
100	90	50
75	75	35
50	50	–

In AMVAR, the 50 ms analysis window gave better estimates of the signal duration when compared to the 150 ms analysis window. Hence, smaller the analysis window (having at least one cycle of the signal) the better is the accuracy of the estimate in the AMVAR method. For multitaper method, a 150 ms window was found to give the best performance. The duration of oscillation as determined by the AMVAR (50 ms analysis window) and the multitaper (150 ms analysis window) methods are tabulated in Table 1. It is clear that the AMVAR method gives a better estimate for the duration of the signal when compared to the multitaper method.

5 Analysis of experimental data

Here, we consider an experiment in which two well trained adult male rhesus macaque monkeys (LU and GE) performed a GO or NO-GO visual pattern discrimination task in experimental sessions of approximately 1,000 trials (Bressler et al. 1993). The experiment was conducted in the Laboratory of Neuropsychology at the National Institute of Mental Health

during 1984–1988 and animal care was in accordance with the institutional guidelines at that time. On each trial the monkeys depressed a hand lever, and kept it pressed during a random interval ranging from 0.12 to 2.2 s (wait period) while waiting for stimulus appearance. On GO trials, a water reward was provided if the monkey released the lever within 500 ms after stimulus onset.

Micro electrodes were implanted in distributed sites that were located in the hemisphere which was contralateral to their dominant hand (left hemisphere in monkey LU and right hemisphere in GE). These were used to record the Local Field Potentials (LFP) in each trial from 14 channels for the time period from −90 to 510 ms. These multivariate LFP time series were sampled at 200 Hz. Combining the LFP recordings from several sessions resulted in a pooled ensemble of many trials for both monkeys.

We consider only the GO trials. This data has been analyzed earlier (Brovelli et al. 2004; Chen et al. 2006; Ledberg et al. 2007). In particular, existence of synchronized beta-frequency (15–30 Hz) oscillations linking different sensorimotor areas to form a large-scale cortical network was established. Further, it was hypothesized that the beta oscillation network in the sensorimotor cortex facilitates the maintenance of steady pressure on the depressed hand lever. Consequently, in GO trials, as the monkey released the hand lever following stimulus presentation, the need to maintain pressure on the lever was removed and the beta oscillation disappeared. This was demonstrated (Zhang et al. 2005) using AMVAR analysis. In our study, we determine the time when the beta oscillation ends for the data recorded from the somatosensory region (channel 6 in monkey LU and channel 8 in monkey GE) using both AMVAR and multitaper methods.

5.1 Data preprocessing

In both methods, for every single trial LFP time series, each amplitude value was divided by the temporal standard deviation to give equal weight to the data from each recording site and trial. The ensemble mean time series from each site was subtracted point wise for each of it's single trial time series. This allows the ensemble of single trial time series to be treated as coming from a zero mean stochastic process. This preprocessing was applied to the LFP recordings of both monkeys.

5.2 Spectral analysis

After data preprocessing, the power spectrum was computed using both methods for each monkey. In the AMVAR method, we used an analysis window of 80 ms with a model order $M = 8$ (40 ms). In multitaper method, we used an analysis

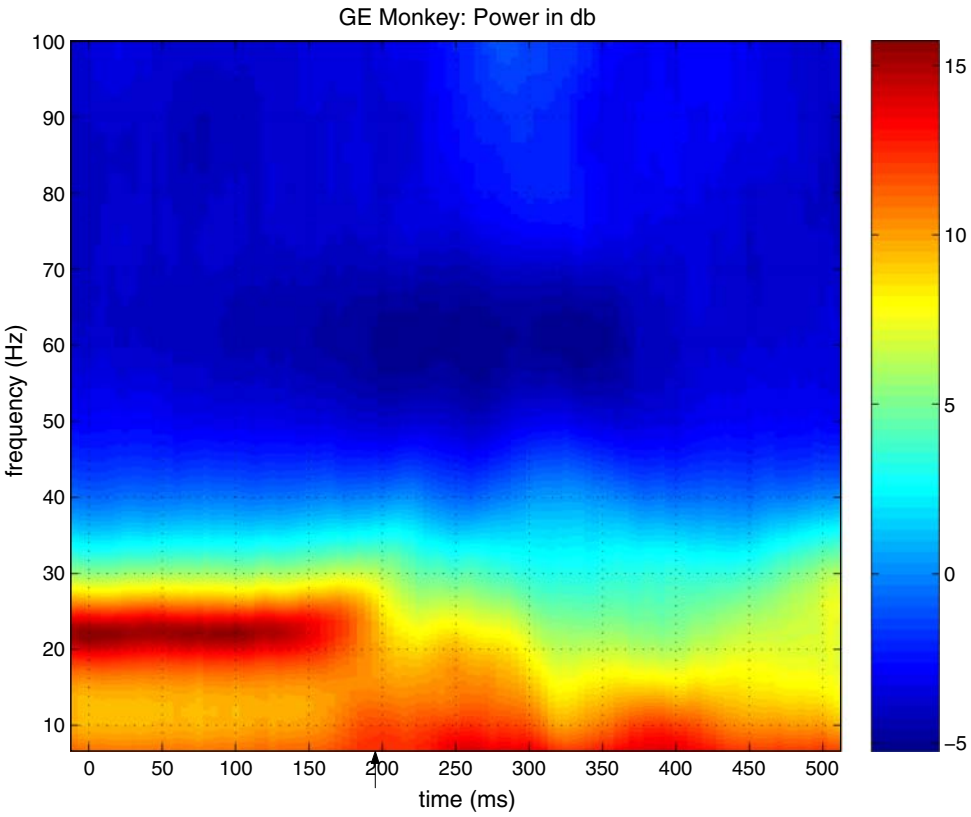

Fig. 8 The time–frequency plot of power spectrum using AMVAR method for monkey GE

window of 150 ms and time bandwidth product $NW\Delta t = 2$ as before.

The power spectrum of full time series data gave a peak around 23 Hz for monkey LU and at 22 Hz for monkey GE by both methods. But when we performed short window spectral analysis by sliding the analysis window (by one data point) along time axis, the multitaper method failed to capture the signal for both monkeys. On the other hand, by the AMVAR method, the peak in the power spectrum appeared right from the first window and terminated at 150 and 190 ms past the start of the signal for monkey LU and GE, respectively. The time–frequency plot of the power spectrum obtained by the AMVAR method for monkey GE is shown in Fig. 8. A similar result (not shown) was found for monkey LU.

6 Discussion

AMVAR and multitaper methods are two widely used methods for spectral analysis of neurobiological data. In this paper, we compared the performance of the two methods using several tests. The AMVAR method performed better compared to multitaper method while estimating the power spectrum for short time series. We demonstrated this by analyzing a short duration simulated signal that was embedded in a background OU noise process. We also showed that, using the AMVAR method, coherence can still be detected in a noisy bivariate time series even though the individual power spectra fail to show any peaks. But, both these methods were immune to jitter in the temporal location of the signal. Performing short window spectral analysis on experimental data, we showed that the AMVAR method was able to detect the termination of beta oscillations in both monkeys LU and GE. On the other hand, the multitaper method failed to capture those oscillations for both monkeys.

For general applications, both AMVAR and multitaper methods are excellent methods for spectral analysis of data. In this paper, for the applications we tested on, the AMVAR method was found to perform better. In other contexts, it is possible that multitaper method is be a better choice. For example, when a power spectrum has complex features or when it is difficult to determine the optimal model order for the AR model, an optimal non-parametric method like the multitaper method is a better choice (Mitra and Pesaran 1999; Dhamala et al. 2008a,b).

Acknowledgments We thank Richard Nakamura, Richard Coppola, and Steve Bressler for providing us with the experimental data used in this study. We also thank Mingzhou Ding and Steve Bressler for useful discussions. GR was supported by DRDO, DST Centre for Mathematical Biology (SR/S4/MS:419/07) and UGC-SAP (Phase IV). He is also associated with the Jawaharlal Nehru Centre for Advanced Scientific Research as a Honorary Faculty Member.

References

Bartosch L (2001) Generation of colured noise. Int J Modern Phys C 12:851–855

Bressler SL, Coppola R, Nakamura R (1993) Episodic multiregional cortical coherence at multiple frequencies during visual task performance. Nature 366:153–156

Brovelli A, Ding M, Ledberg A, Chen Y, Nakamura R, Bressler SL (2004) Beta Oscillations in a large-scale sensorimotor cortical network: Directional influences revealed by Granger causality. PNAS 101:9849–9854

Chen Y, Bressler SL, Ding M (2006) Frequency decomposition of conditional Granger causality and application to multivariate neural field potential data. J Neurosci Methods 150:228–237

Dhamala M, Rangarajan G, Ding M (2008) Estimating Granger causality from Fourier and wavelet transforms of time series data. Phy Rev Lett 100(018701):1–4

Dhamala M, Rangarajan G, Ding M (2008) Analyzing information flow in brain networks with nonparametric Granger causality. NeuroImage 41:354–362

Ding M, Bressler SL, Yang W, Liang H (2000) Short-window spectral analysis of cortical event-related potentials by adaptive multivariate autoregressive modelling: data preprocessing, model validation and variability assessment. Biol Cybern 83:35–45

Gillespie DT (1996) The mathematics of Brownian motion and Johnson noise. Am J Phys 64:225–240

Granger CWJ, Hughes AO (1968) Spectral analysis of short series—a simulation study. J R Stat Soc Ser A 130:83–99

Jenkins GM, Watts DG (1968) Spectral analysis and its applications. Holden Day, San Francisco

Kaminski M, Ding M, Truccolo WA, Bressler SL (2001) Evaluating casual relations in neural systems: Granger causality, directed transfer function and statistical assessment of significance. Biol Cybern 85:145–157

Ledberg A, Bressler SL, Ding M, Coppola R, Nakamura R (2007) Large-scale visuomotor integration in the cerebral cortex. Cereb Cortex 17:44–62

Marple SL (1987) Digital spectral analysis with applications. Prentice Hall, New Jersey

Mitra PP, Pesaran B (1999) Analysis of dynamic brain imaging data. Biophys J 76:691–708

Morf M, Vieira A, Lee D, Kailath T (1978) Recursive multichannel maximum entropy spectral estimation. IEEE Trans Geosci Electron 16:85–94

Muthuswamy J, Thakor NV (1998) Spectral analysis methods for neurological signals. J Neurosci Methods 83:1–14

Percival DB, Walden AT (1993) Spectral analysis for physical applications. Cambridge University Press, New York

Percival D, Walden A (2000) Wavelet methods for time series analysis. Cambridge University Press, Cambridge

Slepian D, Pollak HO (1961) Prolate spheroidal wavefunctions Fourier analysis and uncertainty. I Bell Syst Tech J 40:43–63

Spyers-Ashby JM, Bain PG, Roberts SJ (1998) A comparison of fast fourier transform (FFT) and autoregressive (AR) spectral estimation techniques for the analysis of tremor data. J Neurosci Methods 83:35–43

Thomson DJ (1982) Spectrum estimation and harmonic analysis. Proc IEEE 70:1055–1096

Walden AT (2000) A unified view of multitaper multivariate spectral estimation. Biometrika 87:767–788

Zhang Y, Bressler SL, Chen Y, Nakamura R, Ding M (2005) Beta and gamma synchronization and desynchronization in monkeys during a visual discrimination task. Soc Neurosc Abstr 31 (Prog.No. 413.18)